

Field emission properties of aligned carbon nanotubes grown on stainless steel using CH₄/CO₂ reactant gas

Chien-Liang Lin*, Chia-Fu Chen, Shih-Chen Shi

Department of Materials Science and Engineering, National Chiao Tung University, 1001 Ta Hsueh Road, Hsinchu 30050, Taiwan, ROC

Abstract

Aligned carbon nanotubes (CNTs) were grown on stainless steel 304 by bias-enhanced microwave plasma chemical vapor deposition, using CH₄/CO₂ as the reactant gas. A bias was applied to the microwave plasma to grow the nanotubes over various periods. Experimental results show that well-aligned CNTs grow on stainless steel at a negative bias of -300 V. Energy dispersive spectrometer on TEM indicated that the metal catalyst on the top of the CNTs includes Fe and Ni, but not Cr. The field emission properties of the resultant CNTs were obtained at a negative bias of -300 V: the emission current was $194 \mu\text{A}$ at $2.2 \text{ V}/\mu\text{m}$; and the turn-on voltage, which is the voltage needed to extract current density of $10 \mu\text{A}/\text{cm}^2$, was $1.4 \text{ V}/\mu\text{m}$. © 2003 Elsevier B.V. All rights reserved.

Keywords: Nanotubes; Plasma CVD; High-resolution electron microscopy; Field emission

1. Introduction

Carbon nanotubes (CNTs), since their discovery in 1991 [1], have been considered for use in many different applications. The small dimensions, strength and remarkable physical properties of these materials make them the very promising emitters for field emission devices. Field emission devices based on CNTs have exhibited remarkable emission characteristics and good current stability [2,3], because of the high-aspect-ratio and electrical conductivity, as well as a mechanical stiffness of the nanotubes [4,5].

This study uses the CH₄/CO₂ gas system rather than CH₄/H₂. CH₄/CO₂ can promote the growth rate over that obtained with CH₄/H₂, because of the high concentration of carbon [6]. The growth quality of CNTs has been reported to exceed that of obtained using a conventional reaction in a gas mixture of hydrogen and hydrocarbons [7], and the growth temperature can probably be reduced to under $300 \text{ }^\circ\text{C}$ [8].

In the authors' previous study, CNTs were grown in situ by modified hot filament chemical vapor deposition using an Fe–Cr filament wire (Fe: 72 at.%, Cr: 23 at.%) that acts as a catalyst and a heat source [9]. Furthermore, Okai et al. [10] reported the growth of CNTs on Fe–

Ni–Cr alloy substrate (Fe: 52 wt.%, Cr: 6 wt.%, Ni: 42 wt.%). Comparing, the alloy they used has much less Cr than that of our study. Therefore, in this work, typical stainless steel 304 (Fe: 70 wt.%, Cr: 19 wt.%, Ni: 9 wt.%), an Fe–Ni–Cr alloy with a high Cr content, was used as the substrate to grow CNTs and identify the catalytic effects of the metal. The field emission properties of CNTs grown on the stainless steel were also examined.

2. Experimental details

CNTs were deposited by microwave plasma chemical vapor deposition. The stainless steel 304 had a thickness of 1 mm and an area of $15 \times 15 \text{ mm}^2$. Before deposition, samples were sonicated in acetone for 10 min, washed in DI water and dried using nitrogen gas. Bias-enhanced microwave plasma chemical vapor deposition was used to grow CNTs; various bias conditions and periods were used to grow the CNTs. The reactive gas mixture was CH₄/CO₂ at a flow rate of 30/22.5 sccm. The applied microwave power and pressure were 300 W and 1333 Pa, respectively. No bias, a negative bias voltage -300 V and a positive bias voltage 300 V were separately applied to the substrates to study the effect of the bias on the growth of CNTs on stainless steel 304. CNTs were grown at a bias of -300 V for various periods. An optical pyrometer was used to monitor the temper-

*Corresponding author. Tel.: +886-955979496; fax: +886-3-5504502.

E-mail address: u8818806@cc.nctu.edu.tw (C.-L. Lin).

ature of the substrate, which was maintained at approximately 600 °C.

A scanning electron microscope (SEM) (S-4000, Hitachi) was used to observe the morphology of the growing samples. A Renishaw micro-Raman spectroscope with an argon ion laser (514.5 nm line) was used to characterize the quality of the CNTs. The I – V measurements were made to analyze the field emission properties of the CNTs. Finally, the nanotubes were imaged using a high-resolution transmission electron microscope (HRTEM) (Tecnai 20, Philips), metal catalyst was analyzed using an energy dispersive spectrometer (EDS) attached to the HRTEM.

3. Results and discussion

3.1. Effect of bias on the growth of CNTs

Fig. 1 presents SEM photographs of deposition products grown for 10 min at various biases. The SEM photograph shown in Fig. 1a shows that CNTs grew on stainless steel 304 at a negative bias of -300 V. The surface morphology was almost the same across the entire area. Fig. 1b shows that no CNTs grow on the stainless steel at no bias, and Fig. 1c shows that carbon rods grow on the stainless steel at a positive bias of $+300$ V. However, the morphologies of both samples differed between their corners and the center. Partial surface fragmentation has been reported [11] to produce a wide variety of surface structures, which then translates into a corresponding variety of catalyzed products, ranging from tufts, stumps, to CNTs.

Raman spectroscopy has been used to study multi-wall nanotubes [12]. The first-order Raman spectrum of the CNTs includes strong, sharp peaks at 1581 and 1350/cm, typical of graphitic carbon nanostructures. Fig. 2 presents the Raman spectra of the deposition product grown on stainless steel 304 under various bias conditions for 10 min. As shown in Fig. 2, samples at biases of -300 and $+300$ V yielded two peaks at approximately 1350 and 1581/cm. Furthermore, the Raman spectrum indicates that the sample grown under no bias yielded no carbon structure, as shown in Fig. 1b. From the SEM photographs and Raman spectra, a negative bias of -300 V was selected to examine the various periods of growth of CNTs.

3.2. Various periods of growth of CNTs

Fig. 3 presents SEM photographs of CNTs grown on stainless steel 304 for various periods. Fig. 3a shows the surface breakup of stainless steel 304. The rupture of the surface has been reported [11] to have increased the yield of CNTs and the uniformity of their sizes. According to Fig. 3a–d, the yield and diameter of CNTs increased with the growth time. Besides, vertical CNTs

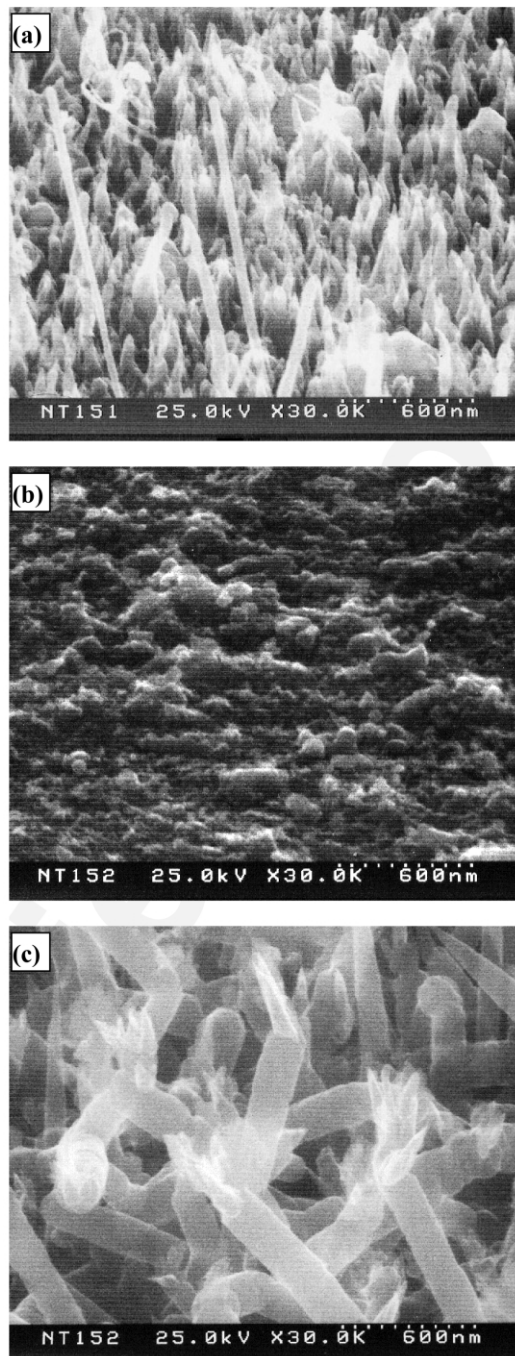


Fig. 1. SEM photographs of deposition product grown on stainless steel 304 at various biases for 10 min; (a) -300 V, (b) 0 V and (c) $+300$ V.

become more prevalent as growth time increases. As shown in Fig. 3d, CNTs grown for 30 min possess a high-aspect-ratio, implying potential use as field emission devices.

Fig. 4 plots the I_D/I_G ratio derived from the Raman spectra obtained after various periods of growth of CNTs on stainless steel 304. The relative intensities of the two peaks depend on the type of graphitic material. As the

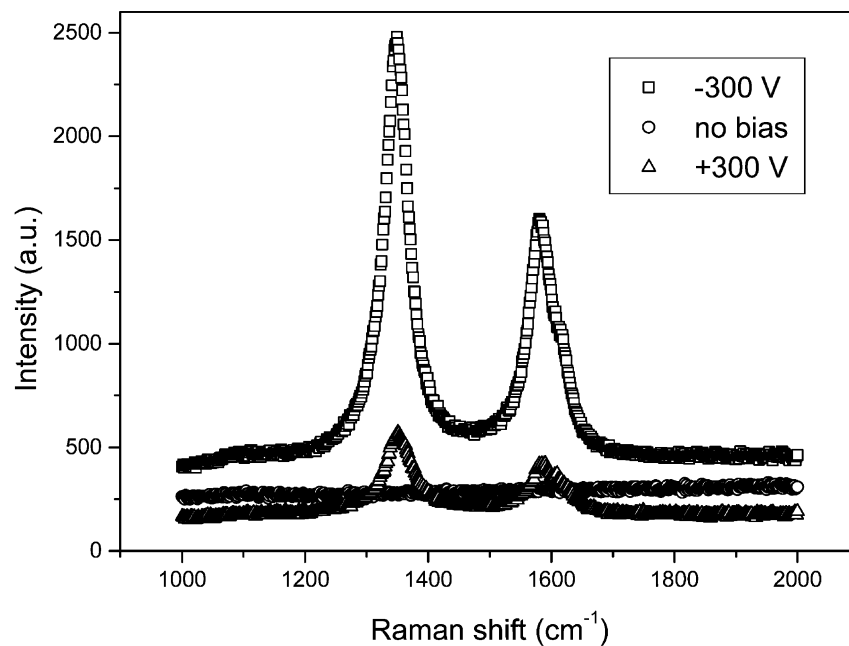


Fig. 2. Raman spectra of deposition product grown on stainless steel 304 at various biases.

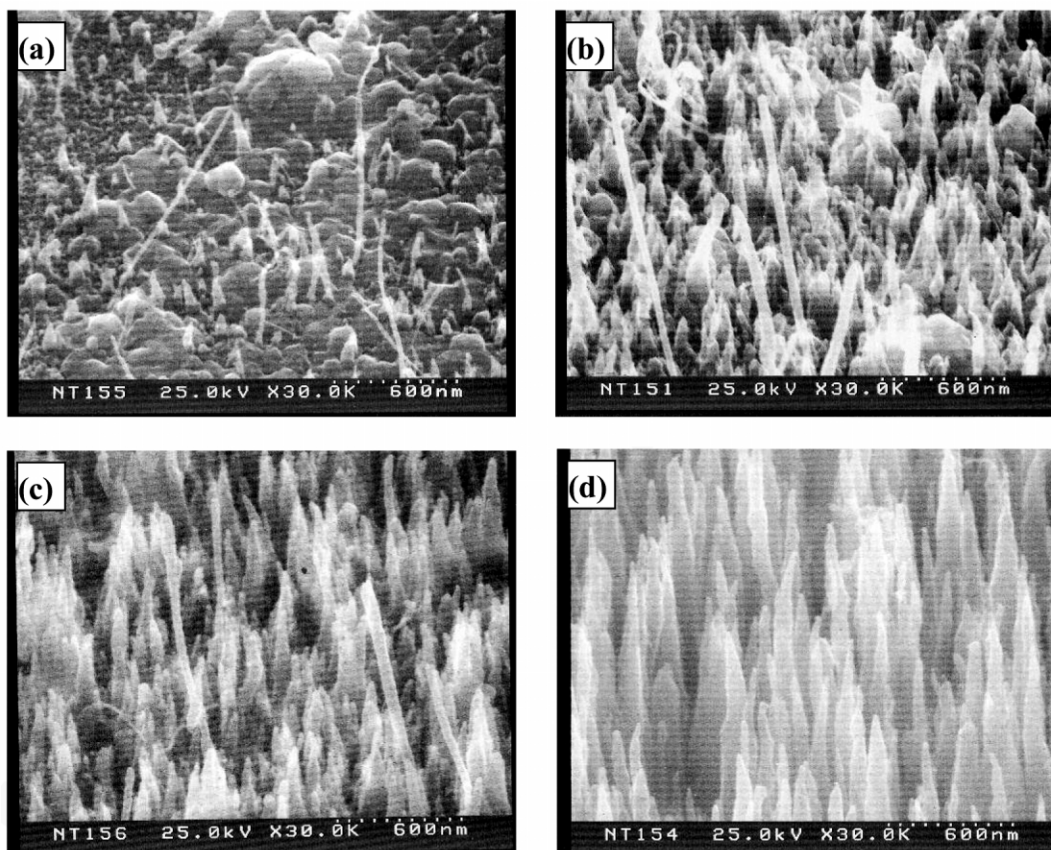


Fig. 3. SEM photographs of CNTs grown on stainless steel 304 for various periods. (a) 5 min; (b) 10 min; (c) 15 min and (d) 30 min.

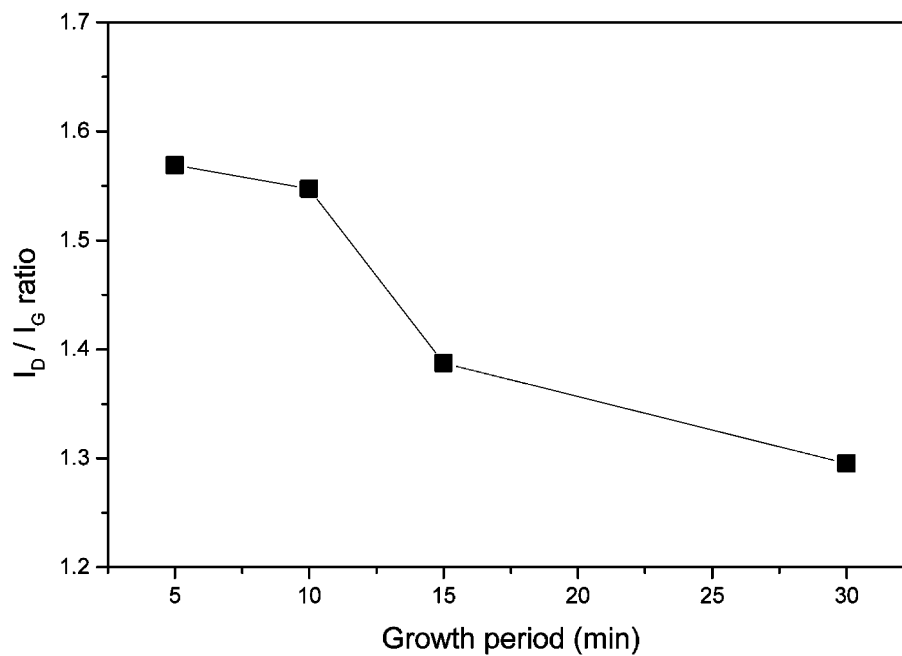


Fig. 4. I_D/I_G ratio derived from Raman spectra of CNTs grown over various periods on stainless steel 304.

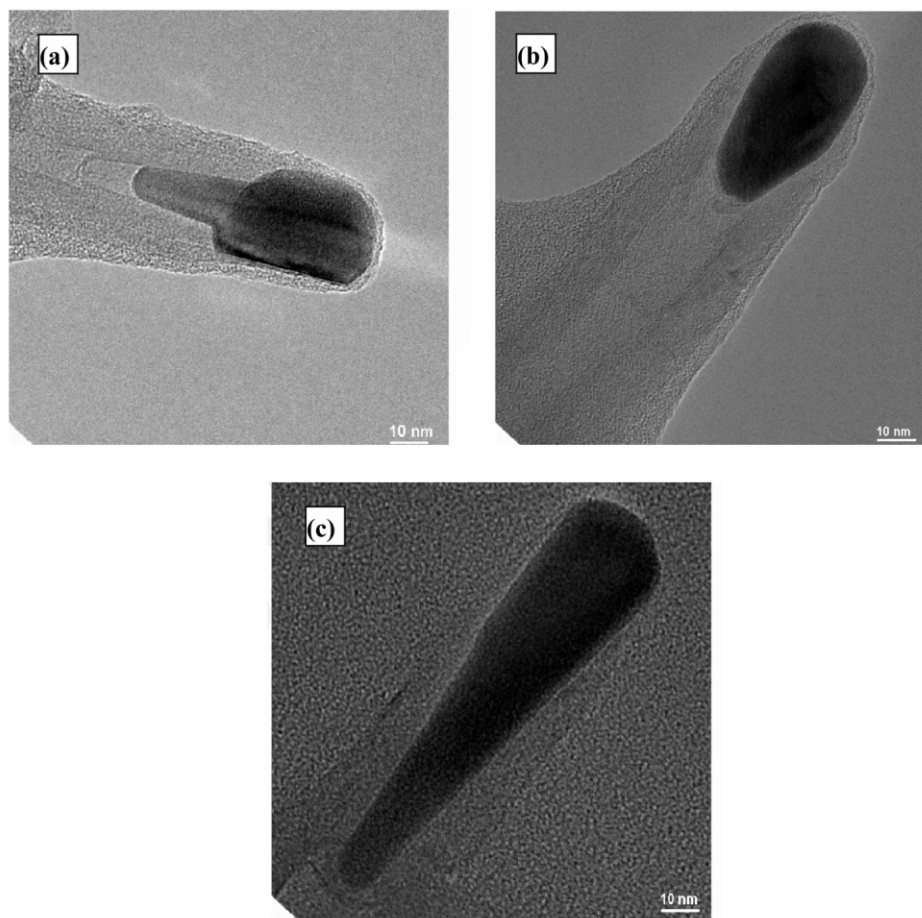


Fig. 5. TEM images of the end section of three individual CNTs grown on stainless steel 304.

Table 1
EDS quantitative analyses of metal catalysts in CNTs

Sample no.	Fe (at.%)	Ni (at.%)	Fe (wt.%)	Ni (wt.%)
1	82.43	17.57	81.70	18.30
2	97.03	2.97	96.89	3.11
3	97.63	2.37	97.51	2.49
4	95.59	4.41	95.37	4.63
5	89.70	10.30	89.23	10.77
6	95.07	4.93	94.83	5.17
7	97.81	2.19	97.71	2.29
8	81.93	18.07	81.18	18.82
9	79.04	20.96	78.20	21.80
10	87.18	12.82	86.61	13.39

ratio of the intensity of the disorder peak at 1335/cm to that of the graphite carbon peak at 1590/cm (I_D/I_G ratio) decreases, the degree of graphitization increases. Fig. 4 shows that the I_D/I_G ratio decreases as the growth period increases. Restated, this figure shows that the crystallinity of the CNTs becomes better as the growth period increases. The SEM photographs show that the product on the samples becomes more uniform and coherent as time passes. The better crystallinity of the CNTs is believed to be attributable to the reduction in the amount of disorganized carbon in the samples.

Fig. 5 shows TEM images of the end section of three individual CNTs. The CNTs were analyzed by TEM to confirm that they were truly CNTs, and not solid carbon fibers. A comparison of these images to those presented elsewhere [8] indicates that the tubes are multi-walled

CNTs. Fig. 5 also reveals that the CNTs have inner diameters of 10–20 nm and outer diameters of 30–40 nm. A comparison of these images with the SEM photograph in Fig. 3d suggests that the catalyst is on the top of the CNTs.

3.3. Catalytic effect of metal

Table 1 presents EDS quantitative analyses of metal catalysts in CNTs. Fig. 5a–c refers to samples 1, 2 and 3, respectively. In these ten samples, EDS signal of Cr is not observed. The top metal particles therefore include only Fe and Ni, but not Cr when the CNTs are grown on the 304 alloy substrate. According to the binary phase diagrams of carbon and metal, the eutectic point of C–Cr alloy is higher than that of C–Fe and C–Ni alloys, which fact is one reason for the elimination of Cr from Fe–Ni–Cr alloy [10]. SEM at low magnification revealed that particles were present along the grain boundary of stainless steel 304. We therefore suggest that chromium carbide is precipitated in the grain boundary of stainless steel at an elevated temperature, in a process similar to that which occurs when stainless steel is heat-treated.

3.4. Field emission properties

The field emission properties of CNTs grown at a –300 V bias for 30 min are obtained using a diode structure. An anode, made of ITO glass, was separated by 500 μm from the tip of a cathode made of CNTs.

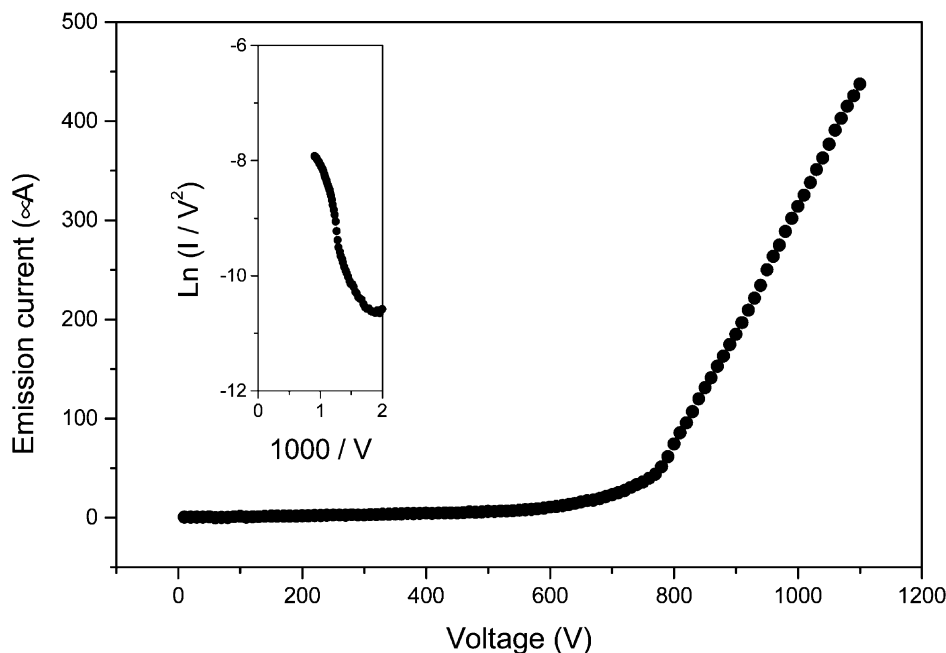


Fig. 6. Emission current against applied voltage, and F–N plot of CNTs grown at –300 V bias for 30 min.

The I – V properties were measured using an electrometer (Keithley 237) and analyzed using the Fowler–Nordheim (F–N) model. Fig. 6 plots emission current against applied voltage, and also presents an F–N plot of this sample. The F–N plot is used to confirm the field emission characteristics. A linear relationship between $\ln(I/V^2)$ and $1000/V$ is obtained. The emission current at an applied voltage of 1100 V ($2.2 \text{ V}/\mu\text{m}$) was $437 \mu\text{A}$ ($194 \mu\text{A}/\text{cm}^2$). The macroscopic turn-on voltage, which is the voltage needed to extract a current density of $10 \mu\text{A}/\text{cm}^2$, was 700 V ($1.4 \text{ V}/\mu\text{m}$).

4. Conclusions

CNTs were grown on stainless steel 304 by microwave plasma chemical vapor deposition using CH_4/CO_2 source gases at a negative bias of -300 V . EDS quantitative analyses indicate that the alloy particles at the top ends of the CNTs have various contents of Fe and Ni. However, Cr was not found at the top of the CNTs, perhaps because the higher eutectic point of C–Cr causes Cr to remain on the substrate and chromium carbide to precipitate on the grain boundary. The field emission properties of the resultant CNTs obtained at a negative bias -300 V were as follows; the emission current was $194 \mu\text{A}$ at $2.2 \text{ V}/\mu\text{m}$, and the turn-on voltage, which is the voltage needed to extract a current density of $10 \mu\text{A}/\text{cm}^2$, was $1.4 \text{ V}/\mu\text{m}$.

Acknowledgments

The authors would like to thank the National Science Council of the Republic of China, Taiwan for financially supporting this work under Contract No. NSC 91-2219-E-009-029.

References

- [1] S. Iijima, *Nature* (London) 354 (1991) 56.
- [2] W.A. de Heer, A. Châtelain, D. Ugarte, *Science* 270 (1995) 1190.
- [3] W. Zhu, C. Bower, O. Zhou, G. Kochanski, S. Jin, *Appl. Phys. Lett.* 75 (1999) 873.
- [4] Z. Yao, C.L. Kane, C. Dekker, *Phys. Rev. Lett.* 84 (2000) 2941.
- [5] E.W. Wong, P.E. Sheehan, C.M. Lieber, *Science* 277 (1997) 1972.
- [6] C.L. Tsai, C.F. Chen, C.L. Lin, *Appl. Phys. Lett.* 80 (2002) 1821.
- [7] M. Chen, C.M. Chen, C.F. Chen, *Thin Solid Films* 420–421 (2002) 203.
- [8] M. Chen, C.M. Chen, S.C. Shi, C.F. Chen, *Jpn J. Appl. Phys.* 42 (2003) 614.
- [9] C.F. Chen, C.L. Lin, C.M. Wang, *Appl. Phys. Lett.* 82 (2003) 2515.
- [10] M. Okai, T. Muneyyochi, T. Yanguchi, S. Sasaki, *Appl. Phys. Lett.* 77 (2000) 3468.
- [11] R.L.V. Wal, L.J. Hall, *Carbon* 41 (2003) 659.
- [12] J. Kastner, T. Pichler, H. Kuzmany, et al., *Chem. Phys. Lett.* 221 (1994) 53.